JOC The Journal of Organic Chemistry

Article

pubs.acs.org/joc

Cyclooctatetraenophanes: A Computational Study

Steven M. Bachrach* and Meghan W. Tang

Department of Chemistry, Trinity University, 1 Trinity Place, San Antonio, Texas 78212, United States

Supporting Information

ABSTRACT: DFT (ωB97X-D, B3LYP-D3, M06-2x, and B3LYP) along with MP2 computations were performed on four cyclophanes composed of two or three cyclooctatetraene (COT) rings connected by two, four, or eight ethylene bridges. Both COT rings in cyclophanes with two ethylene bridges (**2**) and with four bridges in the 1, 2, 5, and 6 positions (**6**) are in a tub conformation. However, the cyclophane with the four bridges in the 1, 3, 5, and 7 positions (**7**) is notable for the near planar geometry of the COT rings. The triple-decker cyclophane **8** has planar top and bottom COT rings, while the central ring is puckered with alternating carbon positions up and down. The nature of the COT rings, especially their antiaromatic character, is assessed using NICS and bond alternation and the distance between the centers of the COT rings.

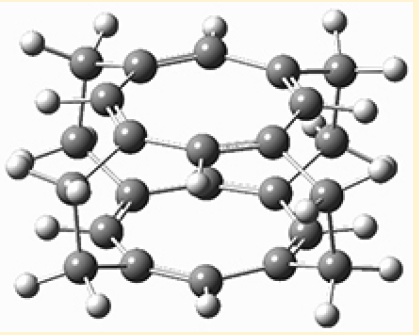

INTRODUCTION

Cyclooctatetraene (COT) has long fascinated organic chemists. Having eight π-electrons, COT is the next larger analogue of benzene with its six π-electrons. The dramatic differences between COT and benzene are rationalized by Hückel's rule. Benzene, having $4n + 2$ π-electrons is aromatic and possesses a planar nonalternant geometry, downfield ^{1}H chemical shifts, and significant stabilization relative to acyclic conjugated polyenes. COT, on the other hand, having $4n$ π-electrons, expresses none of these properties. To avoid the antiaromatic properties associated with $4n$ π-electrons, COT is a nonplanar, alternant polyene. Borden[1] and Lineberger[2] have shown using high-level computations that the D_{8h} geometry of COT is a second-order hilltop; it is the transition state between two D_{4h} geometries which are themselves the transition states for the tub-inversion process.

Cyclophanes are sandwich-like compounds whereby two or more rings are joined by multiple connecting bridges. The exemplar cyclophane is [2.2]paracyclophane (**1**), where two phenyl rings are joined by two ethylene bridges connecting at the *para* positions. Of particular interest with cyclophanes is that they typically induce a strain upon the ring, and can therefore be used to probe the strength of the aromaticity within the ring.

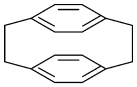

1

Our interest here is to combine these two features, namely, cyclophanes formed of COT rings. Only one such cyclophane has been synthesized; Paquette and Kesselmeyer prepared **2**, where two COT rings are joined at the 1 and 5 positions by ethylene bridges.[3] Their main interest was to examine the possibility of bond-shifting, which interconverts conformers **2a** and **2b**. The X-ray structure analysis revealed just conformer **2a**,[4] consistent with molecular mechanics computations that indicated that **2a** is 3 kcal mol^{-1} lower in energy than **2b**.

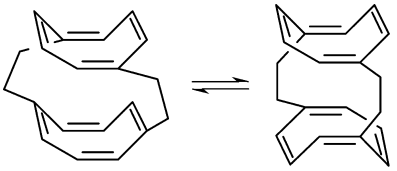

2a **2b**

Whereas cyclophanes formed of phenyl rings act to reduce their aromatic character by bending the rings out-of-plane, the geometric constraints imposed by the bridges connecting COT rings might require the rings to become *more* planar, inducing an antiaromatic character. A number of compounds have been prepared with a planar or near-planar COT core. This is usually accomplished by annulation of multiple rings to COT, such as **3**−**5**.[5−7] We report here a computational study of a variety of cyclophanes formed with two or three COT rings joined by ethylene bridges. These compounds (**2**, **6**, **7**, and **8**) are evaluated for their antiaromatic character using a number of different metrics.

COMPUTATIONAL METHODS

All molecules (the cyclophanes and the reference molecules required to determine strain energies) were optimized for the gas phase within the constraints of point group symmetry where appropriate. To assess the effects of computational methods, optimizations were performed using two different basis sets (6-311G(d) and 6-311+G(2d,p)) and four different density functionals: ωB97X-D,[8] B3LYP-D3,[9−11] M06-2X,[12,13] and B3LYP.[14−17] The first two of these functionals

Received: April 15, 2015
Published: June 12, 2015

DOI: 10.1021/acs.joc.5b00842
J. Org. Chem. 2015, 80, 6679−6686

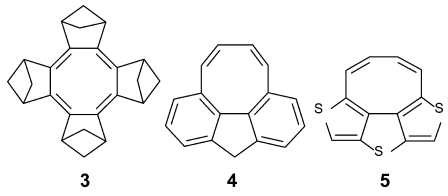

3 4 5

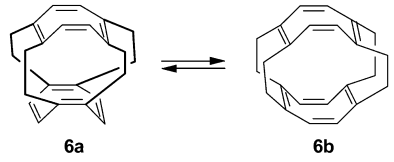

6a 6b

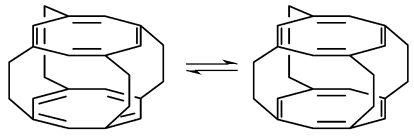

7a 7b

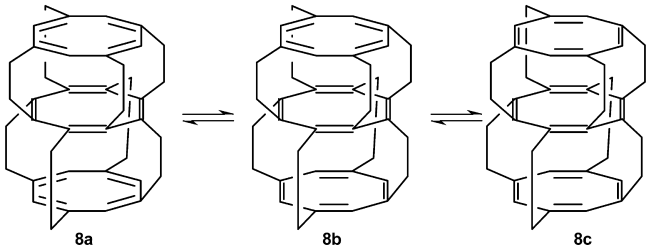

8a 8b 8c

include an explicit correction for dispersion. Though lacking an explicit dispersion correction, the M06-2X functional performs very well with systems with important dispersion contributions.[18,19] Optimizations were also performed at the MP2/6-311G(d) level. Data obtained using the larger 6-311+G(2d,p) basis set are reported in this paper; data with the smaller 6-311G(d) basis set are reported in the Supporting Information, except for the MP2 results, which where only done with the smaller basis set and are reported here.

All structures were confirmed to be local energy minima or transition states by analytical frequency analysis. These frequencies were employed without any scaling factor to compute enthalpy and free energy at 298 K and 1 atm. Strain energies were evaluated using the group equivalent reactions.[20] All computations were conducted using the Gaussian-09 suite.[21]

RESULTS

[2.2.2](1,3,5)Cyclophane (9). To provide a comparison with the COT cyclophanes, we computed the structure of the benzene-based cyclophane [2.2.2](1,3,5)cyclophane (**9**). As with the structure of **1**, the structure of **9** is sensitive to the computational method. The symmetry of **1** has been a topic of some controversy, nicely summarized in the recent study of Wolf et al.[22] Computations of **1** using HF with small basis sets[23,24] and all computations with B3LYP[25−27] predict a D_{2h} structure. However, computations with other functionals, including PBE0,[28] M06-2X,[29] and ωB97X-D,[29] along with MP2[26] and SCS-MP2[26] optimizations predict a structure where the two phenyl rings are twisted with respect to each other into D_2 symmetry. However, the barrier for twisting through the D_{2h} transition state is small. Early crystal structure analysis[30] and an extensive NMR[31] study suggested a D_{2h} ground state. However, Wolf et al. recently published a careful variable-temperature X-ray structure analysis that found that at low temperatures **1** has D_2 symmetry, but it undergoes a phase transition at about 45 K, and above 60 K it appears as a D_{2h} structure.[22]

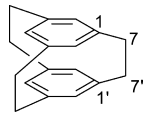

9

B3LYP and B3LYP-D3 with both basis sets predict that **9** has D_{3h} symmetry. Both the D_{3h} and the D_3 structures are predicted to be local minima at the ωB97X-D/6-311+G(2d,p) level. The other methods all predict that the D_{3h} structure is a transition state separating mirror image D_3 structures, where there is a slight twisting about the ethylene groups to avoid the eclipsing interactions of the D_{3h} geometry (see Figure 1). The barrier

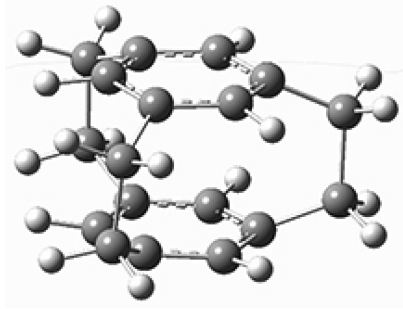

Figure 1. ωB97X-D/6-311+G(2d,p)-optimized geometry of **9** at D_3 symmetry.

represented by the D_{3h} structure is very small, less than 0.1 kcal mol^{-1}. In fact, when zero-point vibrational energy is included, the D_{3h} structure is lower in energy than the D_3 structure, and this is true also when enthalpy is considered. However, the D_3 structure is lower in free energy than the D_{3h} geometry by about 0.5 kcal mol^{-1} (see Table 1). This flat potential energy surface is analogous to what is described above for **1**.

Selected geometric parameters of **9** are listed in Table 1. The computed structures are compared with the X-ray crystal structure.[32] The distance between the centers of the phenyl rings (r_{sep}) is about 2.81 Å in the DFT structures that account for dispersion. The ring separation is longer in the B3LYP structure, which does not account for dispersion. The dihedral angle about the ethylene fragment ($d(C_1C_7C_{7'}C_{1'})$) is small in all structures except for MP2, where it is 10.2°. Overall, the DFT computations are in excellent agreement with the experimental structure.

To assess the strain energy of **9**, we use the group equivalent method,[20] which conserves groups as defined by Benson.[33] The energy associated with eq 1 is the strain energy gained by

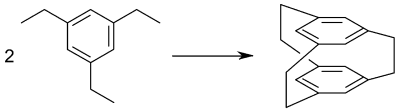

9 Equation 1

making this cage compound. M06-2x and ωB97X-D indicate a strain energy of about 48 kcal mol^{-1}, with that indicated by B3LYP-D3 a bit smaller at 44 kcal mol^{-1}. These values can be compared with the computed strain energy of **1**, which is much smaller at about 30 kcal mol^{-1}.[29] B3LYP overestimates the

DOI: 10.1021/acs.joc.5b00842
J. Org. Chem. 2015, 80, 6679−6686

Table 1. Geometric and Energetic Parameters of 9[a]

	ωB97X-D	B3LYP-D3	M06-2x	B3LYP	MP2	expt[b]
r_{sep}[c]	2.812	2.810	2.805	2.835	2.756	2.790
$d(C_1C_7C_{7'}C_{1'})$[d]	4.8	0.0	6.3	0.0	10.2	0.8
d(ring)[d]	±6.0	±5.6	±5.8	±6.2	±2.8	±6
ΔH[e]	−0.04		−1.08		−0.68	
ΔG[e]	−0.77		0.06		0.41	
strain energy[f]	48.80	44.37	47.74	52.82	37.66	

[a]Using the 6-311+G(2d,p) basis set for the DFT methods and the 6-311G(d) basis set for MP2. [b]Reference 32. [c]Distance between ring centers (Å). [d]In degrees. [e]Barrier through the D_{3h} structure (kcal mol^{-1}). [f]Defined using eq 1, in kilocalories per mole.

strain energy by about 5 kcal mol^{-1}, due to the lack of accounting for dispersion. MP2 seems to exaggerate the aromatic character of the rings in **9**, predicting flatter rings that are closer together than do the DFT methods.

[2.2](1,5)Cyclooctatetraenophane (2). The optimized geometries of **2a** and **2b** are shown in Figure 2. These

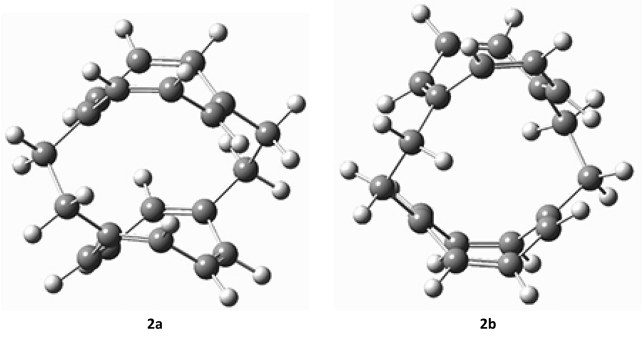

Figure 2. ωB97X-D/6-311+G(2d,p)-optimized geometries of **2a** and **2b**.

conformers are of D_2 and C_2 symmetry, as are the two isomers identified in Paquette's MM study.[4] For all computational levels, **2a** is found to be lower in energy than **2b**, by 6−10 kcal mol^{-1} (see Table 2). This is a larger energy

Table 2. Geometric and Energetic Parameters of 2a and 2b[a]

	ωB97X-D	B3LYP-D3	M06-2x	B3LYP	MP2	expt[b]
r_{sep},[c] **2a**	3.710	3.707	3.676	3.813	3.635	3.719
r_{sep},[c] **2b**	4.047	4.023	4.046	4.073	4.048	
ΔH[d]	7.91	8.18	9.13	6.08	10.09	
strain ethalpy,[e] **2a**	3.07	3.66	2.78	−2.82	6.04	

[a]Using the 6-311+G(2d,p) basis set for the DFT methods and the 6-311G(d) basis set for MP2. [b]Reference 4. [c]Distance between ring centers (Å). [d]Enthalpy difference between **2b** and **2a** (kcal mol^{-1}). [e]Defined using eq 2, in kilocalories per mole.

separation than that predicted by the MM computations, but is consistent with the observation of only a single isomer, **2a**, in the X-ray crystal structure.[4]

The two functionals that account for dispersion (ωB97X-D and B3LYP-D3) give structures very similar to the X-ray structure of **2a**; this can be best identified with the distance between the ring centers (r_{sep}) listed in Table 2. The M06-2x and MP2 structures are slightly contracted, and as expected, B3LYP predicts a structure with the rings too far apart.

The strain energy of **2** can be assessed using the group equivalent reaction shown in eq 2. As might be expected, the

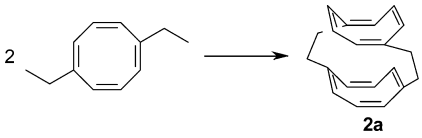

Equation 2

computed strain energy of **2a** is small. All methods (except B3LYP) predict a strain energy of 6 kcal mol^{-1} or less. B3LYP gives an anomalous strain energy of −3 kcal mol^{-1}.

[2.2.2.2](1,2,5,6)Cyclooctatetraenophane (6). Compound **6** has two COT rings joined by four ethylene bridges and, like **2**, can exist as two bond-shift isomers. The optimized structures of these two isomer are shown in Figure 3. In both

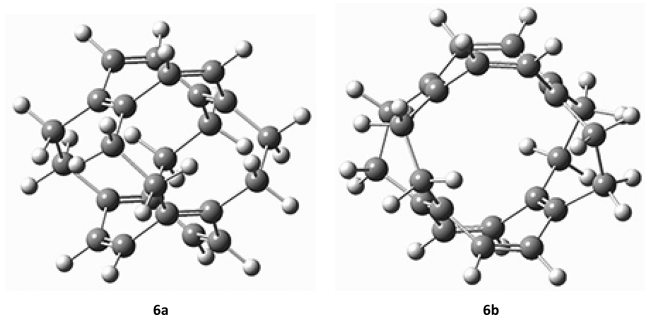

Figure 3. ωB97X-D/6-311+G(2d,p)-optimized geometries of **6a** and **6b**.

isomers, each COT ring remains in a tub conformation. The additional two ethylene bridges do bring the rings closer together in **6** than in **2**. Nonetheless, the COT rings are still much farther apart than are the phenyl rings of **9**.

The difference in enthalpy of these two isomers is about 15 kcal mol^{-1} (Table 3). As with **2**, B3LYP underestimates the

Table 3. Geometric and Energetic Parameters of 6a and 6b[a]

	ωB97X-D	B3LYP-D3	M06-2x	B3LYP	MP2
r_{sep},[b] **6a**	3.677	3.679	3.648	3.731	3.623
r_{sep},[b] **6b**	3.892	3.879	3.888	3.885	3.878
ΔH[c]	14.74	14.19	16.06	7.28	18.23
strain energy,[d] **2a**	−0.70	−3.08	−0.96	−0.24	−8.42

[a]Using the 6-311+G(2d,p) basis set for the DFT methods and the 6-311G(d) basis set for MP2. [b]Distance between ring centers (Å). [c]Enthalpy difference between **6b** and **6a** (kcal mol^{-1}). [d]Defined using eq 3, in kilocalories per mole.

energy difference between the bond shift isomers. For both **2** and **6**, the isomer where the two tubs "stack" (**2a** and **6a**) is more stable than the isomer where the concave faces of each COT ring face each other. Though the rings are joined by two

DOI: 10.1021/acs.joc.5b00842
J. Org. Chem. 2015, 80, 6679−6686

more bridges in **6** than in **2**, the strain energy, as defined by eq 3, is essentially nil, or even slightly negative.

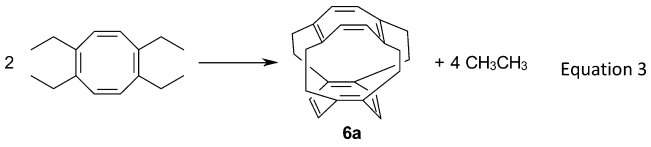

[2.2.2.2](1,3,5,7)Cyclooctatetraenophane (7). An alternative manner for connecting two COT rings with four ethylene bridges is to have them attached at alternating positions, giving rise to **7**. In principle, two different isomers are possible: **7b**, of C_{4h} symmetry, has the double bonds of the top ring aligned (when viewed from above) with the double bonds in the bottom ring, while **7a**, of D_4 symmetry, has the double bonds of the top ring alternating with the double bonds in the bottom ring. A third possibility, **7c**, where the π-electrons delocalize about each ring, is of D_{4h} symmetry.

The ωB97X-D/6-311+G(2d,p) structures of **7a** and **7b** are shown in Figure 4. With both ωB97X-D and M06-2x, **7a** is

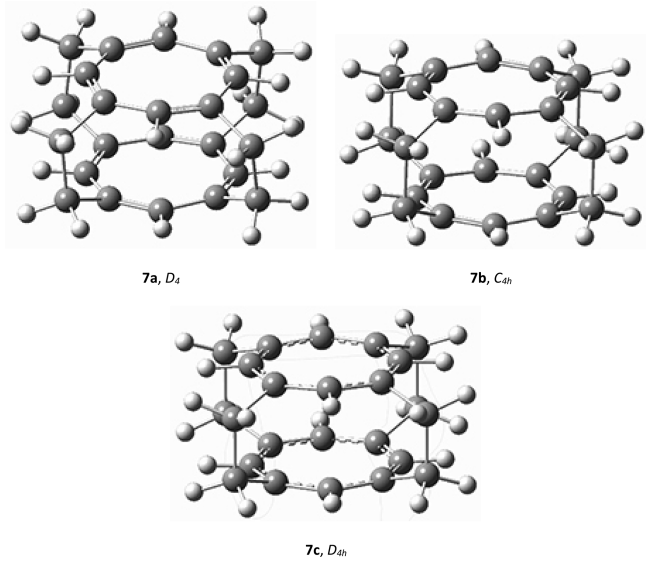

Figure 4. ωB97X-D/6-311+G(2d,p)-optimized geometries of **7a** and **7b** and B3LYP-D3/6-311+G(2d,p)-optimized geometry of **7c**.

lower in energy than **7b**, by 8−9 kcal mol^{-1}. Perhaps the most striking feature of these compounds is that the COT rings are nearly planar. The dihedral angle formed of four consecutive atoms in the COT rings is about ±11.6° in **7a** and ±10.4° in **7b** (see Table 4). There is distinct bond alternation, with differences in C−C single and double bond lengths of 0.114 Å in **7a** and 0.126 Å in **7b**. For comparison, the analogous bond distance difference is 0.143 Å in 1,3,5,7-tetraethylcyclooctatetraene, which has a distinct tub shape. The distance between the centers of the two COT rings is rather small: 2.687 and 2.841 Å in **7a** and **7b**, respectively. This ring separation is much smaller than in **6**; it is even shorter than the distance between the phenyl rings of **9**. The M06-2x structures are very similar to their ωB97X-D counterparts (Table 4).

Optimization of **7a** at MP2 leads to a D_4 structure; however, it displays a lack of bond alternation, with a difference in adjacent C−C bond lengths of only 0.005 Å. The COT rings are nearly planar, with a dihedral angle of four consecutive ring

Table 4. Geometric and Energetic Parameters of 7a−c[a]

	ωB97X-D	B3LYP-D3	M06-2x	B3LYP	MP2
		7a			
r_{sep}[b]	2.687		2.690		2.508
r_{alt}[c]	0.114		0.118		0.005
d(ring)[d]	±11.6		±11.0		±3.9
strain energy[e]	97.52		95.68		56.05
		7b			
r_{sep}[b]	2.841		2.833		
r_{alt}[c]	0.126		0.126		
d(ring)[d]	±10.4		±9.9		
ΔH^f	7.76		9.21		
		7c			
r_{sep}[b]		2.570		2.589	
r_{alt}[c]		0.001		0.000	
d(ring)[d]		8.4		9.0	
strain energy[e]		76.35		85.51	

[a]Using the 6-311+G(2d,p) basis set for the DFT methods and the 6-311G(d) basis set for MP2. [b]Distance between ring centers (Å). [c]Difference in the alternating bond distances in the COT rings (Å). [d]Dihedral angle defined by four successive carbon atoms within the COT ring (deg). [e]Defined using eq 4, in kilocalories per mole.

carbon atoms of only ±3.9°. The distances between the two COT rings is very short, only 2.508 Å. Optimization of the C_{4h} structure inevitably led to the D_{4h} structure **7c**, which is a transition state connecting mirror images of **7a**.

The situation is decidedly different with both the B3LYP and B3LYP-D3 functionals. Optimization with either functional leads to a single isomer, **7c**, with D_{4h} symmetry. It is a true minimum on the potential energy surface, having only real frequencies. Bond alternation is essentially absent, consistent with previous studies that find B3LYP to overemphasize delocalization.[34,35] The rings are not quite planar, with a dihedral angle of four consecutive carbon atoms of about ±9°. The COT rings are close, with a separation of 2.570 Å at the B3LYP-D3 level and 2.589 Å at the B3LYP level.

The strain energy of **7** is evaluated using eq 4. The strain energy divides along the computational method. M06-2x and

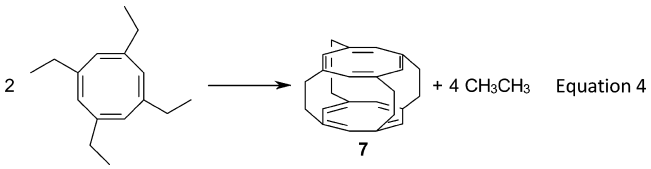

ωB97X-D predict a strain energy that is quite large, about 97 kcal mol^{-1}, as one might expect for a molecule possessing two nearly planar COT rings. B3LYP, which lacks any accounting of dispersion, predicts a strain of 86 kcal mol^{-1}, which is then reduced to 76 kcal mol^{-1} with the inclusion of the D3 correction. Lastly, MP2, which suggests the shortest ring separation, predicts the smallest strain energy of 56 kcal mol^{-1}.

COT Triple-Decker 8. There are three bond-shift isomers of the triple-decker cyclophane formed of three COT rings, with each pair of rings connected by four ethylene bridges. In viewing the molecule from the top, the first isomer, **8a**, has the double bonds in alternating positions, the second isomer, **8b**, has the bottom and center rings with the double bonds aligned while the double bonds in the top ring are not in alignment with the other two rings, and in **8c** the double bonds of all three rings are aligned. For reasons of size, all calculations for **8** were

DOI: 10.1021/acs.joc.5b00842
J. Org. Chem. 2015, 80, 6679−6686

performed with the 6-311G(d) basis set and only with DFT. Since this smaller basis set provided results very similar to those with the larger 6-311+G(2d,p) basis set for **6** and **7** (see the Supporting Information), we expect similarly reliable results for **8**. The ωB97X-D/6-311G(d) structure of **8a** is shown in Figure 5.

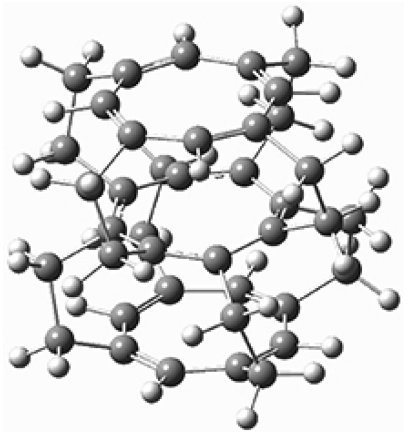

Figure 5. ωB97X-D/6-311G(d)-optimized geometry of **8a**.

All four functionals predict that **8a** is the lowest energy isomer (Table 5). Three functionals predict that **8b** is the next lowest energy isomer, with **8c** as the highest energy isomer; B3LYP-D3 is the outlier with **8c** lower in energy by 2 kcal mol^{-1} than **8b**. M06-2x and ωB97X-D predict that **8b** and **8c** are about 15 and 17 kcal mol^{-1} higher in energy than **8a**, respectively. In addition to differing in the relative order of the isomers, B3LYP-D3 predicts a much smaller range in energy: only 6 kcal mol^{-1} separates the three isomers. B3LYP predicts that **8b** and **8c** are 6 and 20 kcal mol^{-1} above **8a**.

Table 5. Geometric and Energetic Parameters of 8a−c[a]

	ωB97X-D	B3LYP-D3	M06-2x	B3LYP
		8a		
r_{sep}[b]	2.785	2.749	2.782	2.794
r_{alt}[c] (top)	0.113	0.097	0.125	0.100
r_{alt}[c] (center)	0.100	0.060	0.103	0.065
d(ring)[d] (top)	±12.4	±10.6	±12.3	±11.6
d(ring)[d] (center)	±30.1	±27.5	±29.4	±25.3
strain energy[e]	210.73	181.95	205.4	197.39
		8b		
r_{sep}[b]	2.735	2.656	2.740	2.688
	2.889	2.818	2.877	2.873
d(ring)[d] (center)	±30.0	±26.3	±29.3	±28.1
ΔH^f	13.64	6.24	15.37	6.42
		8c		
r_{sep}[b]	2.872	2.729	2.862	2.916
d(ring)[d]	±29.7	±24.4	±29.0	±26.6
ΔH^f	17.22	4.13	17.99	20.52

[a]Using the 6-311+G(2d,p) basis set for the DFT methods and the 6-311G(d) basis set for MP2. [b]Distance between ring centers (Å). [c]Difference in the alternating bond distances in the COT rings (Å). [d]Dihedral angle defined by four successive carbon atoms within the COT ring (deg). [e]Defined using eq 5, in kilocalories per mole. [f]Enthalpy difference (kcal mol^{-1}) relative to **8a**.

The distances separating the COT rings of **8** (Table 5) are slightly longer than in **7**, yet this distance remains quite short; it is less than the distance separating the two phenyl rings in **9**. As with **7**, the top and bottom COT rings are flatter than a typical COT ring. For example, in **8a** the dihedral angle of four adjacent carbon atoms in the top (or bottom) ring is about 10°. However, the central ring in all three isomers is decidedly nonplanar. With all three isomers, and with all four functionals, the dihedral angle of four adjacent carbon atoms of the central ring is about ±30°. Despite the central ring being less planar, the bond alternation is actually less in the central ring of **8a** (0.100 Å at ωB97X-D) than in the top ring (0.113 Å).

The strain energy of **8a** is evaluated using eq 5. Since **8** contains two pairs of linked COT rings, one might expect that

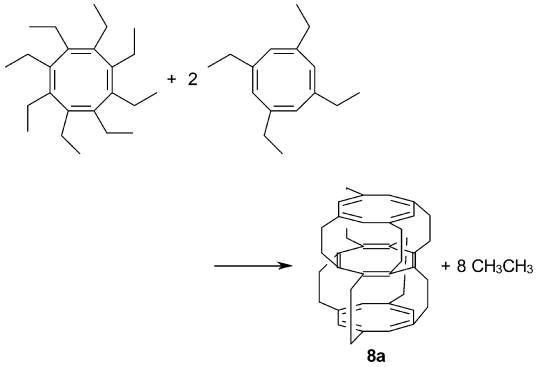

Equation 5

its strain is at least twice that of **7**. In fact, the strain energy of **8** is just slightly greater than twice that of **7**; as an example, ωB97X-D predicts a strain of 211 kcal mol^{-1} for **8** and 98 kcal mol^{-1} for **7**.

DISCUSSION

We begin the discussion by addressing the quality of the computations themselves. Comparison of the computational results is possible with the experimental structures of **2** and **9**. Three important conclusions can be drawn from inspection of Tables 1 and 2, along with the more extensive parameter listings in Tables S1 and S2 (Supporting Information). First, the geometries and strain enthalpies differ in only small ways between the two basis sets, so while we report here the data obtained with the larger 6-311+G(2d,p) basis set, the smaller 6-311G(d) basis set provides nearly identical geometries. This helps to justify the use of the smaller basis set with the much larger triple-decker cyclophane **8**. Second, the three functionals that account for dispersion (ωB97X-D and B3LYP-D3) or midrange dispersion and correlation (M06-2x) provide very similar geometries and strain energies for compounds **2** and **9**. B3LYP, as expected, predicts a ring separation distance that is too long. Both of these patterns are observed with compounds **6**, **7**, and **8** as well. Lastly, the agreement between the computed geometry and the experimental geometry is excellent for both compounds. For example, for **9**, all of the DFT methods properly predict the degree of distortion of the ring from planarity, and the error in the $C_7-C_{7'}$ distance and inter-ring separation is less than 0.02 Å. While some of the DFT methods predict a D_3 ground state and others predict a D_{3h} ground state, and the experiment is only slightly distorted from D_{3h}, all of the functionals indicate a very shallow potential energy surface associated with this rotation. Similar excellent agreement is found between the DFT and experimental structures of **2**. MP2 is a bit of an outlier, predicting a shorter inter-ring separation. These results suggest that these computational methods are

DOI: 10.1021/acs.joc.5b00842
J. Org. Chem. 2015, 80, 6679−6686

appropriate for evaluating the properties and structures of cyclophanes in general.

Compound **2** can exist as two different bond-shift isomers. Both the NMR and X-ray experiments identify a single isomer only: **2a**.[4] All of the computations are consistent with this observation; **2a** is 6−10 kcal mol^{-1} below **2b**. The energy difference at the ωB97XD, B3LYP-D3, and M06-2x levels are clustered around 8 kcal mol^{-1}.

The COT rings in **2** remain in a tub conformation despite being tied together by two ethylene bridges. Perhaps more bridges might distort the ring geometry, but it is not just the number but their arrangement that is critical. Compound **6** has four ethylene bridges in the 1, 2, 5, and 6 positions. These bridges allow each COT ring to remain puckered in the tub conformation. Despite the addition of two bridges, the COT rings of **6** are ever so slightly more puckered than the COT rings in **2** and in 1,2,5,6-tetraethylcyclooctatetraene. This fact, combined with the torsional angle about the ethylene bridges of about 58°, is consistent with a strain energy for **6** that is essentially nil. Thus, **6** appears to be a reasonable synthetic target. The best DFT methods predict that **6a** is 14−16 kcal mol^{-1} lower in enthalpy than **6b**, so like **2**, only one bond-shift isomer will likely be observed.

The structure of **7** is dramatically different from that of **6**: the COT rings of **7** are nearly planar. The dihedral angles formed by four adjacent carbon atoms in the COT rings are about ±11° in **7a** and ±8° in **7b**. Tying together the two COT rings at alternating carbons inhibits the puckering, and the rings are forced to be nearly flat. One might naively then expect that the three COT rings in **8** would also be flat. The top and bottom COT rings are again nearly flat, with dihedral angles of the adjacent four carbon atoms of about 11−12°. However, the central ring is not planar, with analogous dihedral angles in the ring of 28−30°.

While the carbon atoms of the COT rings in **7** are nearly coplanar, the hydrogen or carbon of the ethylenyl group attached to them does not lie near this ring plane. For example, in the ωB97X-D/6-311+G(2d,p) structure of **7a**, the angle formed between the C_1-C_9 bond and the bisector of the $C_2-C_1-C_8$ angle (i.e., the angle between the C_1-C_9 bond and the C_1-B line in Scheme 1) is 165.5°, and the similar angle

Scheme 1. Out-of-Plane Distortion: Angle C_9-C_1-B

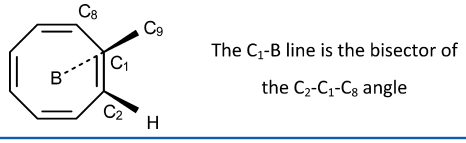

involving the C_2-H bond is 167.9°. Both are tipped in the same direction, toward the other COT ring, a compromise attempt at preserving the planarity of the sp^2 carbon.

The exocyclic carbon must bend toward the other COT ring to form the bridge. For the central COT of **8**, these exocyclic carbons must distort in alternating directions as one goes around the COT ring. Therefore, at C_1, the C_9 carbon must move upward to make the bridge to the top COT ring, but at C_2, the C_{10} carbon must distort downward to make the bridge to the bottom ring. Bending these carbons out of plane is accomplished by both a distortion from planarity about each of the carbons in the central COT ring and also distortion of the ring so alternating ring carbons are moved up or down, destroying the near planarity of the ring.

The near-planar COT rings of **7** and **8** beg the question of the nature of these rings: Might these rings express some aromatic or antiaromatic character? We evaluate this question by examining two properties, the degree of bond alternation around the ring and nucleus-independent chemical shifts (NICSs). For reference, the computed (ωB97X-D) differences in the C−C and C═C bond lengths in cyclooctatetraene and 1,3,5,7-tetraethylcyclooctatetraene are 0.140 and 0.143 Å, respectively, reflecting their nonaromatic/nonantiaromatic character. The bond distance difference is slightly smaller, 0.139 Å, in the planar D_{4h} transition state for the tub inversion of cyclooctatetraene.

NICSs can be computed using Gaussian-09 with the B3LYP and M06-2x functionals only. We therefore report the NICS values using these two methods, along with NICS values obtained using the B3LYP functional on the ωB97X-D geometry. While NICS(1) values are often preferred for evaluating aromaticity, their advantage in our systems is questionable. First, NICS(0) values are thought to be affected by contributions from the σ-electrons in benzene,[36] but since COT is larger than benzene, the σ-contribution will be diminished. Second, the cage environment of the cyclophanes may contribute to the NICS(1) value.

To assess the possible cage affects, we have evaluated NICSs at a series of points along the rotational symmetry axis through the center of the cyclophanes and also for COT (D_{8h}, D_{4h}, and tub) separated by 1 Å. Values for these NICS scans are listed in the Supporting Information. For tub-shaped COT, there is little difference in the NICS values on the concave and convex faces, and this largely reflects the nonaromatic character of this molecule. For **9**, the NICS value monotonically decreases as one moves from the center of the cage, through the center of the phenyl ring and on upward (or downward). For **7** and **8**, the NICS values decrease when moving away from the center of the COT rings, but not with a large difference in the interior versus exterior directions. Given that these NICS scans show small cage effects, we report NICS(0) values primarily, as in Table 6. Since for most of the molecules the NICS(0) values

Table 6. NICS Values (ppm) at Ring and Cage Centers[a]

	B3LYP	M06-2x	B3LYP//ωB97XD
benzene	−7.64	−7.11	−7.64
cyclobutadiene (D_{4h})	−341.57	−171.70	−342.12
cyclobutadiene (D_{2h})	27.01	32.68	27.52
cyclooctatetraene (D_{8h})	−105.76	−79.70	−106.86
cyclooctatetraene (D_{4h})	40.83	36.70	38.49
cyclooctatetraene (D_{2d})	4.85	3.74	3.82
1,3,5,7-tetraethylcyclooctatetraene	2.36	1.98	1.60
9 ring center	−8.44	−7.89	−8.38
9 cage center	−16.36	−17.25	−16.19
7a ring center		11.41	1.97
7a cage center		7.22	−3.60
7c ring center	−22.09		
7c cage center	−32.27		
8a middle ring center	−5.27	−5.14	−3.95
8a top ring center	17.15	−11.87	−10.87

[a]Computed using the 6-311+G(2d,p) basis set except for **8**, for which the 6-311+G(d) basis set was used.

are quantitatively identical for the three methods, by default we will discuss the B3LYP//ωB97X-D value.

The NICS(0) value for planar D_{4h} cyclooctatetraene is 38.5 ppm, a large positive value reflecting its antiaromatic

DOI: 10.1021/acs.joc.5b00842
J. Org. Chem. 2015, 80, 6679−6686

character. The tub geometry has an NICS(0) value that is much smaller, only 3.8 ppm, indicating that antiaromaticity is reduced by moving into the tub geometry. It is worth noting that the highly symmetric D_{8h} structure of cyclooctatetraene and the D_{4h} geometry of cyclobutadiene have spuriously *large and negative* NICS(0) values. Further study of the origins of these unusual NICS values for these highly antiaromatic species, which also happen to be second-order saddle points, is under way.

Turning now to **7**, we see a somewhat divided picture. Both B3LYP and B3LYP-D3 predict that the COT rings of **7** express no bond alternation and the NICS(0) value at the COT ring center (B3LYP) is −22 ppm. This large and negative NICS value is consistent with the spurious value observed for D_{8h} cyclooctatetraene. One must temper any interpretation of these B3LYP results as this functional is prone to overemphasizing π-delocalization.[34,35] The ωB97X-D and M06-2x functionals indicate more bond alternation in the rings of about 0.12 Å than in planar D_{4h} cyclooctatetraene. The M06-2x NICS(0) value of 11.4 ppm suggests some antiaromatic character. The NICS value of 1.97 ppm at B3LYP//ωB97X-D is much more positive than the B3LYP//B3LYP value due to the bond alternation in the ring.

Interpretation of the rings of **8** is equally murky. While the central ring is nonplanar, it shows modest bond alternation (0.1 Å at ωB97X-D and M06-2x, 0.06 Å at B3LYP-D3 and B3LYP) and NICS(0) values that are negative. The top COT ring is nearly planar and expresses a bit more bond alternation than the central ring. However, B3LYP gives a positive NICS(0) value of 17.2 ppm, with M06-2x and B3LYP//ωB97XD giving large negative values.

Therefore, while the NICS analysis does not give an unqualified answer regarding the nature of the cyclooctatetraene rings in **7** or **8**, the inter-ring separation offers an additional perspective. The rings in **7**, **8**, and **9** are connected by ethyl groups, and all things being equal, one might expect the inter-ring separation to be similar in these compounds. However, the inter-ring separation, r_{sep}, in **9** of 2.812 Å (ωB97X-D) is longer than those in **7** (2.687 Å, ωB97X-D) and **8** (2.785 Å, ωB97X-D). Corminboeuf, Schleyer, and Warner[37] have argued that the MOs of the stacked antiaromatic ring may interact such that the degenerate half-filled HOMOs of each antiaromatic ring would mix to create only filled-shell orbitals. A schematic MO diagram for the mixing of the stacked COT HOMOs is shown in Scheme 2. (A full MO diagram of the occupied π-orbitals is presented in the Supporting Information.) This type of MO interaction is stabilizing, and would serve to reduce the antiaromatic character and help stabilize a planar conformation, and these effects are observed in both **7** and **8**. The MO diagram for stacked benzene rings indicated a filled−filled shell interaction of the two HOMOs. Thus, this MO mixing model predicts a shorter inter-ring distance for **7** and **8** than in **9**, consistent with their computed geometries.

Scheme 2. MO Diagram of the Interaction of the HOMOs of COT in a Stacked Arrangement as in 7

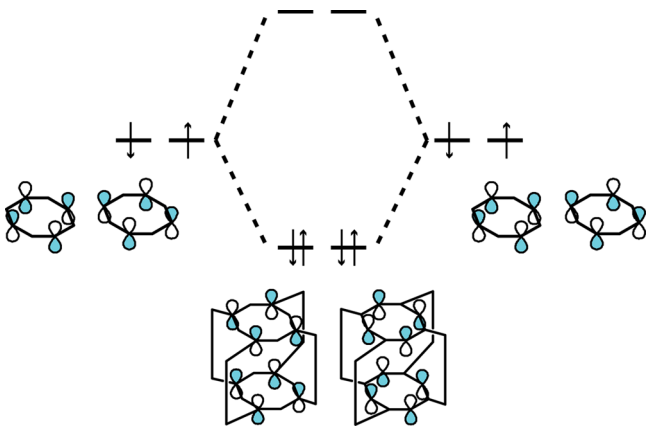

The fact that there is some interaction of the COT rings in **7** begs the question of whether it might be prepared. The strain energy of **7** is moderately large, 97.5 kcal mol^{-1}. This is twice the strain energy of **9**, but not out of the question. For example, the strain of cubane is significantly greater at about 140 kcal mol^{-1}.[38,39] On the other hand, the very large strain energy of **8** (211 kcal mol^{-1}) appears to preclude its possible existence.

CONCLUSIONS

Our computations indicate that cyclophanes formed of cyclooctatetraene rings possess intriguing properties. Cyclophanes **2** and **6** should exist as two bond-shift isomers, with the COT rings in a tub conformation in both isomers. The lower energy isomer has the two COT rings stacked, while the higher energy isomer has the concave faces of the COT rings facing each other. The unfavorable isomer of **6** is of significantly higher energy than the preferred isomer, so experimental identification of this isomer might be difficult. For **2**, only the low-energy isomer **2a** was identified in the NMR and X-ray structure.[4]

Cyclophane **7**, where the four ethylene bridges are attached in alternating positions about the COT ring, has a more striking geometry. The COT rings are nearly planar. Nonetheless, these rings appear to minimize any antiaromatic character. The ωB97X-D and M06-2x structures show moderate bond alternation. The NICS values unfortunately cannot be computed at ωB97X-D, but the M06-2x and B3LYP/ωB97X-D NICS(0) values are small but positive. Most telling is the inter-ring separation: this distance of 2.687 Å is shorter than the separation of the two phenyl rings in **9** (2.812 Å). Even though the bridges in both **7** and **9** are the same length, the rings are not held apart by the same amount. The shorter separation in **7** can be attributed to stabilizing MO interactions between the HOMOs of the COT rings, as opposed to a filled−filled destabilizing interaction between the HOMOs of the phenyl rings of **9**. This MO interaction would also serve to diminish the antiaromatic character of the rings in **7**.

The top and bottom COT rings of the triple-decker cyclophane **8** are, like the rings in **7**, nearly planar. However, the middle COT ring is not planar as the alternating carbon atoms are displaced up or down to allow the ethylene bridges to reach the top and bottom COT rings. This distortion leads to a (unsurprisingly) very large strain energy that is over 200 kcal mol^{-1}. The strain energy of **7** is about 97 kcal mol^{-1}, a not insubstantial strain, but one that can be overcome. We hope that these computations might inspire a synthesis of **7**, a molecule whose structure is certainly interesting and should help us better understand the interplay of strain and antiaromaticity.

ASSOCIATED CONTENT

Supporting Information

Full citation for ref 20, geometric parameters of the cyclophanes (Tables S1−S5), MO diagram of the π-system of **7** (Figures S1), NICS scan values, and coordinates and absolute energies of the cyclophanes. The Supporting Information is

DOI: 10.1021/acs.joc.5b00842
J. Org. Chem. 2015, 80, 6679−6686

available free of charge on the ACS Publications website at DOI: 10.1021/acs.joc.5b00842.

AUTHOR INFORMATION

Corresponding Author

*E-mail: sbachrach@trinity.edu.

Notes

The authors declare no competing financial interest.

ACKNOWLEDGMENTS

We thank the Robert A. Welch Foundation (Grant W-0031) and Trinity University for their support of this research. We also thank a reviewer for helpful comments regarding NICS.

REFERENCES

(1) Hrovat, D. A.; Borden, W. T. *J. Am. Chem. Soc.* **1992**, *114*, 5879−5881.
(2) Kato, S.; Lee, H. S.; Gareyev, R.; Wenthold, P. G.; Lineberger, W. C.; DePuy, C. H.; Bierbaum, V. M. *J. Am. Chem. Soc.* **1997**, *119*, 7863−7864.
(3) Paquette, L. A.; Kesselmayer, M. A. *J. Am. Chem. Soc.* **1990**, *112*, 1258−1259.
(4) Paquette, L. A.; Kesselmayer, M. A.; Underiner, G. E.; House, S. D.; Rogers, R. D.; Meerholz, K.; Heinze, J. *J. Am. Chem. Soc.* **1992**, *114*, 2644−2652.
(5) Matsuura, A.; Komatsu, K. *J. Am. Chem. Soc.* **2001**, *123*, 1768−1769.
(6) Willner, I.; Rabinovitz, M. *J. Org. Chem.* **1980**, *45*, 1628−1633.
(7) Aita, K.; Ohmae, T.; Takase, M.; Nomura, K.; Kimura, H.; Nishinaga, T. *Org. Lett.* **2013**, *15*, 3522−3525.
(8) Chai, J.-D.; Head-Gordon, M. *Phys. Chem. Chem. Phys.* **2008**, *10*, 6615−6620.
(9) Grimme, S.; Antony, J.; Ehrlich, S.; Krieg, H. *J. Chem. Phys.* **2010**, *132*, 154104−154119.
(10) Grimme, S.; Ehrlich, S.; Goerigk, L. *J. Comput. Chem.* **2011**, *32*, 1456−1465.
(11) Becke, A. D.; Johnson, E. R. *J. Chem. Phys.* **2005**, *123*, 154101.
(12) Zhao, Y.; Truhlar, D. G. *Theor. Chem. Acc.* **2008**, *120*, 215−241.
(13) Zhao, Y.; Truhlar, D. G. *Acc. Chem. Res.* **2008**, *41*, 157−167.
(14) Becke, A. D. *J. Chem. Phys.* **1993**, *98*, 5648−5650.
(15) Lee, C.; Yang, W.; Parr, R. G. *Phys. Rev. B* **1988**, *37*, 785−789.
(16) Vosko, S. H.; Wilk, L.; Nusair, M. *Can. J. Phys.* **1980**, *58*, 1200−1211.
(17) Stephens, P. J.; Devlin, F. J.; Chabalowski, C. F.; Frisch, M. J. *J. Phys. Chem.* **1994**, *98*, 11623−11627.
(18) Schreiner, P. R.; Chernish, L. V.; Gunchenko, P. A.; Tikhonchuk, E. Y.; Hausmann, H.; Serafin, M.; Schlecht, S.; Dahl, J. E. P.; Carlson, R. M. K.; Fokin, A. A. *Nature* **2011**, *477*, 308−311.
(19) Hansen, A.; Bannwarth, C.; Grimme, S.; Petrović, P.; Werlé, C.; Djukic, J.-P. *ChemistryOpen* **2014**, *3*, 177−189.
(20) Bachrach, S. M. *J. Chem. Educ.* **1990**, *67*, 907−908.
(21) Frisch, M. J.; et al. *Gaussian-09*, revision D.01; Gaussian, Inc.: Wallingford, CT, 2009.
(22) Wolf, H.; Leusser, D.; R. V. Jørgensen, M.; Herbst-Irmer, R.; Chen, Y.-S.; Scheidt, E.-W.; Scherer, W.; Iversen, B. B.; Stalke, D. *Chem.—Eur. J.* **2014**, *20*, 7048−7053.
(23) Canuto, S.; Zerner, M. C. *Chem. Phys. Lett.* **1989**, *157*, 353−358.
(24) Shen, T. L.; Jackson, J. E.; Yeh, J. H.; Nocera, D. G.; Leroi, G. E. *Chem. Phys. Lett.* **1992**, *191*, 149−156.
(25) Walden, S. E.; Glatzhofer, D. T. *J. Phys. Chem. A* **1997**, *101*, 8233−8241.
(26) Grimme, S. *Chem.—Eur. J.* **2004**, *10*, 3423−3429.
(27) Caramori, G. F.; Galembeck, S. E.; Laali, K. K. *J. Org. Chem.* **2005**, *70*, 3242−3250.
(28) Kamya, P. R. N.; Muchall, H. M. *J. Phys. Chem. A* **2008**, *112*, 13691−13698.
(29) Bachrach, S. M. *J. Phys. Chem. A* **2011**, *115*, 2396−2401.
(30) Hope, H.; Bernstein, J.; Trueblood, K. N. *Acta Crystallogr., B* **1972**, *28*, 1733−1743.
(31) Dodziuk, H.; Szymański, S.; Jaźwiński, J.; Ostrowski, M.; Demissie, T. B.; Ruud, K.; Kuś, P.; Hopf, H.; Lin, S.-T. *J. Phys. Chem. A* **2011**, *115*, 10638−10649.
(32) Hanson, A. W. *Cryst. Struct. Commun.* **1980**, *9*, 1243−1247.
(33) Benson, S. W. *Thermochemical Kinetics*; 2nd ed.; Wiley-Interscience: New York, 1976.
(34) Woodcock, H. L.; Schaefer, H. F.; Schreiner, P. R. *J. Phys. Chem. A* **2002**, *106*, 11923−11931.
(35) Rzepa, H. S.; Sanderson, N. *Phys. Chem. Chem. Phys.* **2004**, *6*, 310−313.
(36) Schleyer, P. v. R.; Jiao, H.; van Eikema Hommes, N. J. R.; Malkin, V. G.; Malkina, O. L. *J. Am. Chem. Soc.* **1997**, *119*, 12669−12670.
(37) Corminboeuf, C.; Schleyer, P. v. R.; Warner, P. *Org. Lett.* **2007**, *9*, 3263−3266.
(38) Bachrach, S. M. *J. Phys. Chem. A* **2003**, *107*, 4957−4961.
(39) Eaton, P. E. *Angew. Chem., Int. Ed. Engl.* **1992**, *31*, 1421−1436.

DOI: 10.1021/acs.joc.5b00842
J. Org. Chem. 2015, 80, 6679−6686